ANU-P/1065
January 1991

TRANSIENT FIELD MEASUREMENTS OF g-FACTORS IN ^{194,196,198}Pt; $g(2_1^+)$ SYSTEMATICS IN TRANSITIONAL W, Os, Pt NUCLEI

A.E. STUCHBERY
Department of Nuclear Physics. Research School of Physical Sciences and Engineering
Australian National University, GPO Box 4, Canberra ACT 2601, Australia

G.J. LAMPARD AND H.H. BOLOTIN
School of Physics, University of Melbourne, Parkville, Vic 3052, Australia

Accepted for publication in Nuclear Physics A
January 1991
ANU P/1065

TRANSIENT FIELD MEASUREMENTS OF g-FACTORS IN ^{194,196,198}Pt; $g(2_1^+)$ SYSTEMATICS IN TRANSITIONAL W, Os, Pt NUCLEI

A.E. STUCHBERY

Department of Nuclear Physics, Research School of Physical Sciences, Australian National University, GPO Box 4, Canberra, ACT 2601 Australia

G.J. LAMPARD* and H.H. BOLOTIN

School of Physics, University of Melbourne, Parkville, Vic 3052, Australia

* Present address: Telecom Research Laboratories, 770 Blackburn Rd, Clayton, Victoria 3168

Abstract: Transient field precessions were measured simultaneously for levels in the nuclei $^{182,184,186}W$ and $^{194,196,198}Pt$ as their ions traversed polarized Gd hosts. These results allow a critical evaluation of conflicting g-factor values reported previously for the even Pt isotopes. Mass variations of $g(2_1^+)$ in the even W, Os, Pt nuclei are examined using the proton-neutron interacting boson model (IBM-2). The measured g-factors depart from the simplest IBM-2 description perhaps due to subshell effects and/or small contributions from non-collective configurations which cause the neutron-boson g-factor to vary with mass.

NUCLEAR REACTIONS $^{182,184,186}W(^{37}Cl, ^{37}Cl')$, $^{182,184,186}W(^{58}Ni,^{58}Ni')$, $^{194,196,198}Pt$ $(^{37}Cl,^{37}Cl')$, $^{194,196,198}Pt(^{58}Ni,^{58}Ni')$, $E_{Cl} = 115$ MeV, $E_{N_i} = 160$ MeV, natural targets; measured $W(\theta,H,T)$ in polarised Gd, particle-γ coin., Coulomb excitation, thin-foil transient-field IMPAC technique. Measured transient-field precessions W Gd, Pt Gd. ^{186}W, $^{194,196,198}Pt$ levels deduced g.

NUCLEAR STRUCTURE $^{180,182,184,186}W$, $^{186,188,190,192}Os$, $^{192,194,196,198}Pt$ calculated g, interacting boson model.

1. Introduction

One of the successes of the proton-neutron interacting boson model has been its ability to describe the mass-dependent systematics of the g-factors of the first 2^+ states in medium and heavy mass nuclei[1-3]. Near A = 190, however, there are indications of structure [1,3,4] in the $g(2_1^+)$ systematics not accounted for by the global interacting boson model descriptions [1-3]. Unfortunately, theoretical investigations of the g-factor systematics in this mass region have been impeded by discrepant experimental values of the 2_1^+ level g-factors in several isotopes of Pt.

About a decade ago Levy et al.[5] performed measurements of the g-factors of the 2_1^+ states in ^{194}Pt and ^{196}Pt using thin-foil, transient-field techniques with polarized Fe hosts. They calibrated the transient field (TF) strength for Pt ions traversing Fe using measured precessions for states in the nuclei ^{186,188}Os which had independently determined g-factors. The gyromagnetic ratios extracted for the states in ^{194,196}Pt using this calibration of the TF for Fe hosts were significantly smaller than prior static-field implantation and radioactivity measurements. Levy et al.[5] attributed the disparity between their TF study and previous static field studies to possible systematic errors in the static-field measurements. The alternative, that both the static-field and TF measurements are correct, but that there is a discontinuity in the strength of the TF between $_{76}$Os and $_{78}$Pt was dismissed by Levy et al.[5]. However, this alternate interpretation has been investigated in detail over the past decade and experimental results [6-11] as well as theoretical considerations [7,10] point to diminished TF strengths for Pt ions in Fe compared with Os ions in Fe when the ion velocities are about $2v_0$ ($v_0 = c/137$, the Bohr velocity). While the evidence for this discontinuity in the TF strength is considerable, it is still criticised occasionally [12]. The present measurements were undertaken with the aim of removing further contention as to the

values of the g-factors of the 2_1^+ states in ^{194,196,198}Pt. Along with the nuclear structure interest in these quantities, to be discussed below, our interest was also rekindled by the need for suitable accurate calibration gyromagnetic ratios for our recently completed experimental study [13] of g-factors in ^{195}Pt.

2. Experimental Design

As the present work, in part, aims to resolve discrepancies between g-factors measured for states in Pt isotopes using transient-field and other techniques, we could not utilize a previously measured g-factor of a level in an isotope of Pt to calibrate the TF strength for Pt ions. Instead, an extrapolation of the TF measured for tungsten ions (Z = 74) was relied upon. As no discontinuities in TF strength for ions with neighbouring atomic numbers have been observed [8,14,15] for heavy ions traversing Gd hosts, nor are any anticipated [11,16] for ions near Z=78, we have measured TF precessions simultaneously for excited states in ^{194,196,198}Pt and ^{182,184,186}W as their ions traversed polarized Gd foils. Simultaneous measurements such as these, in which the nuclei being studied (^{194,196,198}Pt) and those used to calibrate the TF(^{182,184,186}W) traverse the same polarized ferromagnetic foil, largely obviate possible sources of systematic error. A similar experimental approach was taken in our study [11,16] of g-factors in ^{197}Au.

To broaden the scope for verification of our measured g-factors we performed two runs, the essential difference between them being that during the first (Run I) the W and Pt ions traversed the ferromagnetic Gd host at a lower average velocity than during the second (Run II).

3. Experimental Procedures and Analysis

3.1 EXPERIMENTAL PROCEDURES

Beams of ^{37}Cl at 115 MeV (Run I) and ^{58}Ni at 160 MeV (Run II) from the Australian National University 14UD Pelletron accelerator were used to Coulomb excite states of interest in $^{182,184,186}W$ and $^{194,196,198}Pt$. The target used for both runs consisted of an annealed Gd foil, 4.2 ± 0.2 mg cm^{-2} thick, on the upstream side of which was sputtered, first, 0.65 ± 0.04 mg cm^{-2} of natural W, and then, 0.94 ± 0.05 mg cm^{-2} of natural Pt (i.e. incident projectiles encountered the Pt layer first). A layer of natural Cu ~7 mg cm^{-2} thick, sufficient to stop the recoiling W and Pt ions, was evaporated on the downstream side of the Gd foil. This multi-layered target was then pressed onto a 15 μm thick Cu backing, using an indium flashing as adhesive, to provide added mechanical support and improved heat conduction away from the beam spot. Target layer thicknesses were determined by areal-weight measurements and Rutherford scattering and energy-loss measurements using 7 and 8 MeV alpha particles from the University of Melbourne 5U Pelletron accelerator.

Two pairs of Ge detectors were placed at ±65° and ±115° to the beam direction and used to register γ-rays in coincidence with backscattered beam ions detected in a common annular silicon surface-barrier detector (151° – 168°). This coincidence requirement restricted data acquisition to events associated with W and Pt ions recoiling through Gd within forward cones of mean half angles ~9° (Cl beam; Run I) and ~8° (Ni beam; Run II). The average times for W and Pt ions to traverse the various target layers and the energies with which these ions entered into and emerged from the Gd layer are summarized in table 1.

The Gd foil was polarized by an external magnetic field of 0.05T applied in a direction normal to the reaction plane and its sense was reversed

automatically at frequent intervals. Beam bending effects were rendered negligible by a soft-iron cone located between the target and annular detector.

The target was cooled using liquid nitrogen and maintained at a temperature of ~90K while beam was on target. Other aspects of the thin-foil transient field techniques used have been described in earlier publications [17-19].

Particle-γ-ray angular correlations were measured for each bombardment, the most statistically precise data being taken during Run I using the 115 MeV ^{37}Cl beam. During these measurements, the two backward-quadrant detectors were left at ±115° to serve as monitors while the forward detectors were placed, in turn, at several angles between 0° and ±65° to the incident beam direction.

The γ-ray detector efficiencies were determined by placing ^{152}Eu and ^{182}Ta sources at the target position.

3.2 ANALYSIS OF DATA

Procedures employed to extract g-factors from measured TF precessions, in which account is taken of the effects of cascade feeding and decay in flight, have been outlined elsewhere [17-19]. In the present study corrections for levels decaying whilst the ions were in motion through the Gd foil were negligible for all states of interest. Although the measured g-factors [20-24] of the corresponding low-lying levels of the stable even ^{182,184,186}W isotopes are not the same, previous measurements [21-24] have established that the low-lying levels in the ground-band (gsb) of any given one of these isotopes have identical g-factors within experimental uncertainties. As these isotopes were included for the purpose of calibrating the TF strength, there was no need to extract the separate contributions to the observed (raw)

precessions of the individual gsb levels in any individual even W isotope studied. Rather the time-integrated TF strength experienced by W ions was inferred directly from the observed cascade-fed precessions [e.g. see ref. [25]] in each separate case.

On the other hand, small contributions to the observed precessions of the 2_1^+ levels populated via decays from the 2_2^+ and 4_1^+ states in the nuclei ^{194,196,198}Pt had to be taken into account. Since the populations of the 2_2^+ and 4_1^+ levels were small relative to those of the 2_1^+ levels (of the order of 5%) in each nucleus and for both runs, the corrected precessions for the 2_2^+ levels obtained from a detailed analysis including previous measurements [17,26,27] of the ratios $g(2_2^+) / g(2_1^+)$ and $g(4_1^+) / g(2_1^+)$, did not differ significantly from those extracted using a simpler analysis in which these g-factor ratios were assumed to be unity within each Pt nuclide.

4. Experimental Results

A representative spectrum of backscattered ^{58}Ni beam ions registered in coincidence with de-excitation γ-rays during Run II is shown in fig. 1. Similar particle spectra were obtained during Run I. Figure 2 displays the gamma-ray spectra recorded at 65° in coincidence with the separate W and Pt target strata regions indicated in fig. 1. The relatively good separation of the particle groups backscattered from the contiguous W and Pt target layers simplified the data analysis.

Representative measured and calculated unperturbed particle-γ-ray angular correlations for various transitions in the W and Pt isotopes are displayed for Run I in fig. 3 and for Run II in fig. 4.

Transient field precession angles measured for states in ^{182,184,186}W during Runs I and II are summarized in table 2, while the TF precession angles measured for states in ^{194,196,198}Pt are presented in table 3.

5. Transient Field Calibration and Deduced g-factors

5.1 TRANSIENT FIELD CALIBRATION

While the extraction of the *relative* gyromagnetic ratios of the 2_1^+ levels in ^{194,196,198}Pt from the simultaneously measured TF precessions shown in table 3 is straightforward, to obtain the *absolute* g-factors of these levels from the observed precession angles requires a determination of the velocity-dependent magnitude of the TF for Pt ions recoiling through polarized Gd. As noted above (sect. 2), and in prior publications [8,9,14-16], no abrupt discontinuity in the behaviour of the TF strength as a function of atomic number is expected [11,16] or observed [8,14,15] for ions with atomic numbers between 54 and 88 traversing Gd. Measured TF strengths for W ions in Gd have been found [8,11,16] to be in accord with the Chalk River parametrization of the TF strength which also describes its strength for ions of lower [14] and higher [15] atomic number traversing Gd.

In light of the foregoing, the absolute values of the gyromagnetic ratios of the 2_1^+ states of ^{194,196,198}Pt were obtained from the precessions measured in Gd by scaling the TF strengths *simultaneously* measured for W ions traversing the same host foil with virtually the same recoil velocities. Corrections were made for the slightly different velocity ranges with which the W and Pt ions traversed the Gd foil and for the atomic number dependence of the TF strength using the Chalk River parametrization [14,15]. The calculated correction factors were, for Run I (II) : ϕ (Pt<u>Gd</u>) / ϕ (W<u>Gd</u>) = 1.103(1.106), where $\phi \equiv \Delta\theta/g$.

To assess the sensitivity of the extracted g-factors to the assumed velocity dependence of the TF, these correction factors were re-calculated taking the TF to have (i) a linear dependence on ion velocity, and (ii) a constant value, independent of ion velocity. As these "extreme" cases yielded correction factors that differed by approximately 4.5% from those adopted, we

assign a systematic uncertainty of ± 4.5% to the correction factors for each of the runs.

Whereas the gyromagnetic ratios adopted here for the low-lying ground-band states in ^{182,184}W are the same as those discussed and adopted in previous work [9,11,16,23], that taken for the lowest ground-band states in ^{186}W differs from our earlier work [9,11,16,22]. As noted previously [9], there are conflicting values for $g(2_1^+, ^{186}W)$ in the literature [20]. In particular, two PAC measurements [20], both giving g = 0.36 ± 0.02, appear to conflict with the Mössbauer result [28] g=0.312±0.011. In earlier work [9] we attempted to discriminate between these conflicting values for $g(2_1^+)$ in ^{186}W using the well-known value of $g(2_1^+)$ in ^{184}W and measurements of the ratio $g(2_1^+; ^{186}W) / g(2_1^+; ^{184}W)$ obtained in TF studies. However, the bulk of the data then available were not obtained during simultaneous measurements and as such are superseded by the present results (table 2) and results reported in refs. [11,16]. From table 2 and refs.[11,16] we obtain $g(2_1^+; ^{186}W) / g(2_1^+; ^{184}W) = 1.067 \pm 0.052$. Together with the adopted value [21] of $g(2_1^+; ^{184}W)$ this yields $g(2_1^+; ^{184}W) = 0.308 \pm 0.017$ in excellent agreement with the Mössbauer value [28] which we adopt in the following analysis. [It may be noted that this value is somewhat smaller than that taken earlier [9,11,16,22], implying some rescaling of previous results may be required; however in refs [11,16] the changes are significantly smaller than the experimental uncertainties in the adopted g-factors.]

For the relative measurements of precessions of states in the W and Pt nuclei reported here, the absolute magnitudes of the TF precession angles are not of critical importance. However, we note that while the precessions we measured for WGd in facets of earlier work [11,16] were in agreement with the predictions of the Chalk River parametrization [14,15], those measured in the current study were diminished to ~66% of that expected. In this case the reduction could be anticipated as the only target available to us had to be prepared using a Gd foil that had been annealed poorly. Although this

situation was not ideal the experiments were designed so that the results would be independent of the foil magnetization and the conclusions of the present work are not affected.

5.2 g-FACTORS IN ^{194,196,198}Pt

Gyromagnetic ratio results for the 2_1^+ states of ^{194,196,198}Pt obtained in the present measurements are summarised in table 3. It can be concluded readily from the results of both Run I and Run II that the g-factors of the 2_1^+ states in ^{194,196,198}Pt are the same within experimental uncertainties. However, while the absolute g-factor results from both runs agree within the assigned errors (table 3), those measured during Run I are about 10% smaller than those from Run II (i.e. at the limit of the one-standard-deviation errors). It is not clear whether this is due to random errors entirely or indicates some systematic deviation. It will be evident from comparisons made in the following section that the results of Runs I and II are no more disparate than some of the previously reported static field results and that the magnitude of the difference is not sufficient to weaken the conclusions of the present work. Nevertheless, we carefully and critically examined our experimental procedures and re-evaluated the data to seek possible sources of systematic error. Our conclusion is that *if* there is any systematic difference between the results of Runs I and II, it almost certainly comes about in the extrapolation of the TF strength for Pt in Gd from that measured simultaneously for W ions in Gd. As can be seen from table 1, the Pt and W ions sampled the TF at lower average velocities during Run I ($\langle v/v_0 \rangle \sim 2$) than during Run II ($\langle v/v_0 \rangle \sim 3$) and in both runs the Pt ions moved more slowly than the W ions. If the dependence of the TF on ion velocity were closer to linear than the Chalk River parametrization[14,15] predicts at ion velocities around $2v_0$ and/or nearer to constant than it predicts at velocities near $3v_0$ (both plausible), then the apparent disparity between the g-factor results from Runs I and II would be

reduced. Since appropriate estimates of such systematic uncertainties in the TF calibration procedure have been included already in the errors assigned to the g-factors in table 3, and also, as the differences between the results of Run I and Run II may after all be random in nature, an option might be to adopt for $g(2_1^+)$ in ^{194,196,198}Pt the weighted average of the g-factors from Runs I and II. However, we make a more conservative estimate of the errors and assign the arithmetic average of the errors from Runs I and II to the weighted average g-factor values shown in the final column of table 3.

5.3 COMPARISON OF RESULTS

The present measured gyromagnetic ratios in ^{194,196,198}Pt are compared with previous static-field and transient-field measurements in table 4. The lifetime-dependent static-field results shown have been corrected for mean life values listed in the compilation of Raman et al [29]. The IMPAC results of Kalish et al [31] were corrected for a TF contribution to the observed precession angles and re-evaluated using the internal field for Pt Fe adopted by Garber et al [32].

With the exception of the g-factor for ^{194}Pt reported by Berkes et al [30] (obtained by re-evaluating the weighted average of prior work), the static-field g-factor results shown in table 4 are in agreement. Katayama et al [26] have discussed possible reasons for discrepancies between various IPAC studies of $g(2^+)$ in ^{194}Pt and ascribe the smaller g-factors obtained in some measurements to insufficient magnetic polarization of the ^{194}Ir Fe sources used. It should be noted that the results for $g(2^+)$ in ^{194}Pt and ^{196}Pt compiled by Berkes et al [30] are from different original works and that, in contrast with the measurements for ^{194}Pt, those for ^{196}Pt employ ^{196}Au Fe sources. There

would be no incongruity, therefore, in accepting the result reported by Berkes et al [30] for ^{196}Pt while rejecting that for ^{194}Pt.

The present TF g-factor results for ^{194,196,198}Pt obtained relative to previously determined g-factors in ^{182,184,186}W agree well with the static field values. Relative g-factor values from the present and prior TF studies are also in excellent agreement. Only the absolute g-factors obtained in ref [5] by, in effect, extrapolating the TF strength for Pt Fe from that of Os Fe are in marked disagreement with both the present TF values and the prior static-field measurements. As many groups have measured [7,17,18,27,35-38] TF precessions for Pt in Fe hosts that confirm the experimental precessions reported by Levy et al [5], there must be a significantly smaller TF strength for Pt in Fe than they presumed in extracting the g-factors of the first-excited states of ^{194,196}Pt. This discontinuity in TF strength between Os and Pt has been discussed in several previous publications [7,9-11].

6. Discussion

As noted in the introduction, the proton-neutron interacting boson model (IBM-2) has been successful in describing the qualitative mass-dependent systematics of $g(2_1^+)$ in medium and heavy mass even-even nuclei [1-3]. If the 2_1^+ levels in even nuclei are assumed to be symmetrical in the proton and neutron degrees of freedom (i.e. the states have maximum F-spin), then

$$g(2_1^+) = g_\pi (N_\pi/N_t) + g_\nu(N_\nu/N_t), \qquad (1)$$

where $g_\pi(g_\nu)$ are proton (neutron) boson g-factors, $N_\pi(N_\nu)$ are proton (neutron) boson numbers and $N_t = N_\pi + N_\nu$. While the collective model estimate for the gyromagnetic ratio, $g \sim Z/A$, always shows a monotonic decrease with increasing mass for a sequence of isotopes, eq. (1) can show an increase with

neutron number, as is often observed in nuclei where the major shells are more than half full. It can be noted that eq. (1) agrees with the estimate Z/A for $g_\pi = 1$ and $g_\nu = 0$ only if Z and A are regarded as effective numbers of valence nucleons.

For graphical presentation, it is useful [39] to rewrite eq. (1) as

$$g(2_1^+) = g_+ + g_- \ (N_\pi - N_\nu)/N_t, \qquad (2)$$

where $g_\pm = (g_\pi \pm g_\nu)/2$. In this form, a plot of $g(2_1^+)$ against $(N_\pi - N_\nu)/N_t$ will be a straight line unless the underlying microscopic structure of the proton and neutron bosons changes markedly through the mass region of interest.

Measured [14,20,21] $g(2_1^+)$ values for the isotopes $^{180\text{-}186}$W, $^{186\text{-}192}$Os and $^{192\text{-}198}$Pt are plotted as a function of $(N_\pi - N_\nu)/N_t$ in figure 5. The near constancy of $g(2_1^+)$ in $^{192\text{-}198}$Pt is in striking contrast with the increases in $g(2_1^+)$ with mass observed for ^{180}W – ^{192}Os. Results of least-squares fits of eq. (1) to the combined data and for the isotopes of each atomic number separately are displayed in fig. 5 and summarised in table 5. Also included in table 5 are the results of the fit performed by Wolf, Casten and Warner [3] for 16 nuclei between ^{176}Hf and ^{198}Pt with which the current combined fit agrees. Clearly, the quality of the fit to the combined data is poor whereas better fits are obtained when different values of the boson g-factors are allowed for each atomic number. The most dramatic change in these fitted values of g_π and g_ν takes place between the isotopes of Os and those of Pt. For $^{180\text{-}186}$W and $^{186\text{-}192}$Os g_π and g_ν are near the values expected [1,2] by assuming only the orbital angular momenta of the fermions contribute to the boson g-factors (i.e. $g_\pi \simeq 1$ and $g_\nu \simeq 0$). For the Pt isotopes, however, $g_\pi \simeq g_\nu \simeq 0.3$.

Since the nuclear shape changes [40] from prolate to oblate between ^{192}Os and ^{192}Pt, the underlying single-particle structure of the bosons might be expected to change and cause changes in g_π and g_ν. Moreover, on the basis of

the systematics of the energy ratio $E(4_1^+)/E(2_1^+)$, and other theoretical considerations, Casten [41] has drawn attention to a subshell closure at N = 114 effective for Z ≥ 78. In the IBM-2 such changes in the underlying fermion structure can be related to the changes in the $g(2_1^+)$ systematics (i) through [1,2] the boson g-factors g_π and g_ν, and/or, (ii) through [3] effective numbers of proton and neutron bosons, N_π^{eff}, N_ν^{eff}. An analysis [3,42,43] of $g(2_1^+)$ systematics in terms of effective numbers of proton and neutron bosons has proved useful in the A = 150 region to elucidate the presence of a subshell closure at Z = 64 for N≤88. Wolf and Casten [43] extracted both N_π^{eff} and N_ν^{eff} from the measured $g(2_1^+)$ and $B(E2; 2_1^+ \rightarrow 0_1^+)$ values for each nucleus of interest by solving simultaneously eq. (1) and the approximate analytical expression [ref. [44]]:

$$B(E2; 2_1^+ \rightarrow 0_1^+) = 0.25\,(1 - 0.1\chi)^2\,[(N_t + 1)/N_t]^2\,(e_\nu N_\nu + e_\pi N_\pi)^2, \qquad (3)$$

where $e_{\pi(\nu)}$ are the proton (neutron) boson effective charges and χ is the parameter of the quadrupole operator. In their analysis the boson charges and boson g-factors were assumed constant and mass-dependent variations of the g-factors and B(E2)s were attributed entirely to changes in the effective numbers of bosons.

We performed a similar analysis for the isotopes ^{192}Pt to ^{198}Pt. The values of g_π (g_ν) were fixed from the fit to $g(2_1^+)$ in ^{180}W through ^{192}Os (see table 5) and $e_\pi = 0.22 \pm 0.01$, $e_\nu = 0.08 \pm 0.01$ determined by a fit of eq. (3) to the measured [29] B(E2)s in the same nuclei. These boson charges agree with those of ref. [3]. As the results are not very sensitive to the value of χ chosen we followed Wolf and Casten [43] and took χ = -0.05 for all W, Os and Pt nuclei studied.

The deduced effective neutron boson numbers for ^{192}Pt to ^{198}Pt are shown in the upper panel of fig. 6 along with lines indicating the boson numbers obtained by counting from the closed shell at N = 126 and the proposed subshell closure at N = 114. Effective proton-boson numbers are shown in the lower panel. There is no clear manifestation of a subshell effect

at N = 114 in the effective boson numbers displayed in fig. 6. A subshell effect would be expected to give values of N_ν^{eff} lying between those obtained by conventional counting from N=126 and those counted from N=114, but the extracted values are larger than both. Similarly, the significant departures of N_π^{eff} from $N_\pi = 2$, and its variations with mass, are not anticipated and cannot be easily related to changes in the fermion sub-shell structure.

Evidently the transitional structures of the A~190 nuclei are more complex than those of the nuclei near A = 150 and the assumption that the boson parameters, e_π, e_ν, g_ν and g_ν, applicable for ^{180}W to ^{192}Os are appropriate also for $^{192\text{-}198}Pt$ is not valid. It is of note that a fit of eq. (3) to the B(E2) data for $^{192\text{-}198}Pt$ using conventional boson counting yields a good fit with $e_\pi = 0.22 \pm 0.02$ and $e_\nu = 0.010 \pm 0.01$; i.e. the proton charge is similar to that for ^{180}W - ^{192}Os but the neutron charge is about 20% larger in $^{192\text{-}198}Pt$. Effective boson numbers extracted for $^{192\text{-}198}Pt$ with the increased neutron-boson charge are also shown in fig. 6. These effective numbers of bosons are closer to those obtained by conventional counting (as they must be) but the unexpected mass dependence of N_ν^{eff} remains and the fitted value of $N_\nu^{eff} \simeq 4$ for ^{198}Pt seems too large as $N_\nu = 3$ for this nucleus whether one counts from N = 126 or N = 114. These difficulties suggest that a more useful interpretation may emerge if g_ν is allowed to vary from isotope to isotope for $^{192\text{-}198}Pt$.

While the above analysis does not clearly indicate any fermion subshell effects at N = 114, neither does it exclude the possibility that such effects may be present if the boson charges and boson g-factors also vary with mass. Unfortunately we do not have sufficient experimental information to determine all relevant parameters. To proceed, therefore, we have assumed $g_\pi = 0.90$ and $e_\pi = 0.22$ for $^{192\text{-}198}Pt$ and sought the values of N_ν and g_ν required to reproduce the B(E2) and $g(2_1^+)$ data for various assumed values of e_ν and N_π^{eff}. Results for two cases are presented in fig. 7. In these and all other fits performed with reasonable assumed values for N_π^{eff} and e_ν the

inferred values of N_ν^{eff} were generally nearer those obtained by conventional counting and g_ν always showed a pronounced monotonic decrease from ^{192}Pt to ^{198}Pt. It seems unambiguous from this analysis that the observed near-constant $g(2_1^+)$ values in $^{192\text{-}198}$Pt can be related to a mass-dependent diminishing of the neutron-boson g-factor, g_ν.

It may be significant that in the weakly oblate Pt nuclides the $\nu 1i_{13/2}$ orbital [g = -0.18, ref. [45]] is nearly full and the $\nu 3p_{3/2}$ orbital [g = -0.82, ref. [45]] is close to the Fermi surface. A small contribution to the neutron d-boson from the term $(\nu 3p_{3/2})^2_{2^+}$ which increases with mass number, for example, could explain the observed trend in $g(2_1^+)$ for $^{192\text{-}198}$Pt. This would imply that the spin contributions to g_ν do not cancel altogether and suggest that the 2_1^+ states of the heavier Pt isotopes may have a small non-collective component (less than a few percent) in their structures – a reasonable suggestion since the $g(2_1^+)$ values for $^{198\text{-}204}$Hg apparently manifest larger non-collective effects [46]. Also, it may require non-collective effects to explain the observed variations [18,22,23] between $g(2_1^+)$ and $g(2_2^+)$ in ^{184,186}W and ^{188,192}Os which cannot be accounted for readily by collective models [4].

Finally, we note that the *departures* of the measured 2_1^+-state g-factors in ^{196,198}Pt from the global IBM-2 fit track consistently with variations of the relative pairing gaps for protons and neutrons in these nuclei. As estimated from odd-even mass differences, the relative pairing gap Δ_n/Δ_p diminishes more rapidly from ^{192}Pt to ^{198}Pt than it does for ^{180}W to ^{186}W or ^{186}Os to ^{192}Os. (For the W isotopes it actually increases slightly.) As a decrease in Δ_n/Δ_p is usually associated with an increase in the proportion of the nuclear angular momentum carried by the neutrons it also generally implies a smaller g-factor. Clearly, detailed calculations are required to elucidate the relative import of the fermion level structure (subshell effects) and non-collective single-particle configurations in determining the g-factors and pair-field strengths.

7. Summary and Conclusion

Precise measurements were made of the 2_1^+ level g-factors in ^{194,196,198}Pt relative to previously determined g-factors in ^{182,184,186}W using transient field techniques. The TF precessions were measured simultaneously as ions of W and Pt traversed polarized Gd hosts. The g-factors measured are in excellent agreement with results from radioactivity and implantation studies using static hyperfine fields. Our results confirm a smaller transient field strength for Pt in Fe than for lighter neighbouring ions traversing Fe.

Gyromagnetic ratios of the 2_1^+ levels in 16 nuclei between ^{180}W and ^{198}Pt are not described well by a global fit using the simplest IBM-2 formula [eq. (1)]. In particular, the $g(2_1^+)$ values in ^{196}Pt and ^{198}Pt are smaller than predicted by the overall fit. The diminution of these g-factors may be brought about by a combination of subshell effects near N = 114 and small non-collective contributions to the wavefunctions.

Acknowledgements

The authors wish to express their appreciation for the support and cooperation of the staff of the Australian National University 14UD Pelletron Laboratory. The aid of Mr B. Szymanski and Mr A.H.F. Muggleton in facets of target preparation is acknowledged with thanks as is the aid of V.Y. Hansper and A.J. Morton in the target thickness measurement. One of us (GJL) acknowledges the support of an Australian Post-Graduate Award.

References

1. M. Sambataro, O. Scholten, A.E.L. Dieperink and G. Piccitto, Nucl. Phys. **A423** (1984) 333.

2. P. van Isacker, K. Heyde, J. Jolie and A. Sevrin, Annals of Physics **171** (1986) 253.

3. A. Wolf, R.F. Casten and D.D. Warner, Phys. Lett. **B190** (1987) 19.

4. A.E. Stuchbery, in Proceedings of the international conference on nuclear structure through static and dynamic moments, Vol. II, p.153, ed. H.H. Bolotin, Melbourne, Conference Proceedings Press, 1987; and references therein.

5. R. Levy, N. Tsoupas, N.K. B. Shu, A. Lopez-Garcia, W. Andrejtscheff and N. Benczer-Koller, Phys. Rev. **C25** (1982) 293.

6. A.E. Stuchbery, C.G. Ryan, H. Ohnuma, G.B. Beard and H.H. Bolotin, Phys. Rev. **C27** (1983) 434.

7. A.E. Stuchbery, C.G. Ryan and H.H. Bolotin, Hyperfine Interact. **13** (1983) 275.

8. D. Bazzacco, F. Brandolini, K. Loewenich, P. Pavan, C. Rossi-Alvarez,R. Zannoni and M. de Poli, Phys. Rev. **C33** (1986) 1785.

9. A.E. Stuchbery, H.H. Bolotin and C.E. Doran, Hyperfine Interact. **36** (1987) 117.

10. A.E. Stuchbery, Hyperfine Interact. **39** (1988) 199.

11. A.E. Stuchbery, H.H. Bolotin, A.P. Byrne, C.E. Doran and G.J. Lampard, Z. Phys. **A330** (1988) 131.

12. N. Benczer-Koller, D.J. Ballon and A. Pakau, Hyperfine Interact. **33** (1987) 37.

13. G.J. Lampard, A.E. Stuchbery and H.H. Bolotin, to be published.

14. O. Häusser, H.R. Andrews, D. Ward, N. Rud, P. Taras, R. Nicole, J. Keinonen, P. Skensved and C.V. Stager, Nucl. Phys. **A406** (1983) 339.

15. O. Häusser, H.R. Andrews, D. Horn, M.A. Lone, P. Taras, P. Skensved, R.M. Diamond, M.A. Deleplanque, E.L. Dines, A.C. Macchiavelli and F.S. Stephens, Nucl. Phys. **A412** (1984) 141.

16. A.E. Stuchbery, L.D. Wood, H.H. Bolotin, C.E. Doran, I. Morrison, A.P. Byrne and G.J. Lampard, Nucl. Phys. **A486** (1988) 374.

17. A.E. Stuchbery, C.G. Ryan, H.H. Bolotin, I. Morrison and S.H. Sie, Nucl. Phys. **A365** (1981) 317; A.E. Stuchbery, Ph.D. Thesis, University of Melbourne, 1982, unpublished.

18. A.E. Stuchbery, I. Morrison, L.D. Wood, R.A. Bark, H. Yamada and H.H. Bolotin, Nucl. Phys. **A435** (1985) 635.

19. A.P. Byrne, A.E. Stuchbery, H.H. Bolotin, C.E. Doran and G.J. Lampard, Nucl. Phys. **A466** (1987) 419.

20. Table of isotopes, 7th edn., ed. C.M. Lederer and V.S. Shirley (Wiley, New York, 1978) appendix VII.

21. A. Alzner, D. Best, E. Bodenstedt, B. Gemünden, T. Merzhäuser, H. Reif, R. Trzcinski, R. Vianden and U. Wrede, Z. Phys. **A316** (1984) 87.

22. A.E. Stuchbery, H.H. Bolotin, C.E. Doran, I. Morrison, L.D. Wood and H. Yamada, Z. Phys. **A320** (1985) 669.

23. A.E. Stuchbery, H.H. Bolotin, C.E. Doran and A.P. Byrne, Z. Phys. **A322** (1985) 287.

24. G.J. Lampard, A.E. Stuchbery, A.P. Byrne, C.E. Doran and H.H. Bolotin, unpublished data.

25. A.E. Stuchbery, C.G. Ryan, H.H. Bolotin and S.H. Sie, Phys. Rev. **C23** (1981) 1618.

26. I. Katayama, S. Morinobu and H.Ikegami, Hyperfine Interact. **1** (1975) 113.

27. A.E. Stuchbery, C.G. Ryan, I. Morrison and H.H. Bolotin, Phys. Rev. **C24** (1981) 2106.

28. B. Persson, H. Blumberg and D. Agresti, Phys. Rev. **170** (1968) 1066.

29. S. Raman, C.H. Malarkey, W.J. Milner, C.W. Nestor, Jr. and P.H. Stelson, Atomic Data and Nucl. Data Tables **36** (1987) 1.

30. I. Berkes, R. Roughny, M. Mayer-Lévy, P. Chéry, J. Danière, G.Lhersonneau and A. Troncy, Phys. Rev. **C6** (1972) 1098; and refs. therein.

31. R. Kalish, L. Grodzins, R.R. Borchers, J.D. Bronson and B. Herskind, Phys. Rev. **161** (1967) 1196.

32. D.A. Garber, M. Behar, Z.W. Grabowski and Wm.C. King, Z. Phys. **270** (1974) 163.

33. M. Kawamura, T. Tomiyama and H. Kato, Journal Phys. Soc. Japan **50** (1981) 1832.

34. O. Häusser, B. Haas, D. Ward and H.R. Andrews, Nucl. Phys. **A314** (1979) 161.

35. N.K.B. Shu, D. Melnick, J.M. Brennan, W. Semmler and N. Benczer-Koller, Phys. Rev. **C21** (1980) 1828.

36. A.E. Stuchbery, C.G. Ryan and H.H. Bolotin, Phys. Rev. **C24** (1981) 1480.

37. R. Kalish, N.K.B. Shu, N. Benczer-Koller, A. Holthuizen, A.J. Rutten, F.A. Becker and G. Van Middelkoop, Hyperfine Interact. **8** (1980) 151.

38. J. de Raedt, J. Billowes, A. Pakou and M.A. Grace, Hyperfine Interact. **9** (1981) 507.

39. I. Morrison, Australian Journal of Fhysics **33** (1980) 801.

40. G.J. Gyapong, R.H. Spear, M.T. Esat, M.P. Fewell, A.M. Baxter and S.M. Burnett, Nucl. Phys. **A458** (1986) 165; C.S. Lim, R.H Spear, W.J. Vermeer, M.P. Fewell and G.J. Gyapong, Nucl. Phys. **A485** (1988) 399.

41. R.F. Casten, Nucl. Phys. **A443** (1985) 1.

42. A. Wolf, D.D. Warner and N. Benczer-Koller, Phys. Lett. **158B** (1985) 7.

43. A. Wolf and R.F. Casten, Phys. Rev. **C36** (1987) 851.

44. R.F. Casten and A. Wolf, Phys. Rev. **C35** (1987) 1156.

45. R. Bauer, J. Speth, V. Klemt, P. Ring, E. Werner and T. Yamazaki, Nucl. Phys. **A209** (1973) 535.

46. W.R. Kölbl, J. Billowes, J. Burde, M.A. Grace and A. Pakou, Nucl. Phys. **A448** (1986) 123.

TABLE 1

Experimental Kinematics: Transit Times and Energies of Recoiling Ions Traversing Target Strata.

Run; Beam	Target Ion	T_{Pt}[a] (ps)	T_W[a] (ps)	T_{Gd}[a] (ps)	E_i[a] (MeV)	E_e[b] (MeV)	v_i/v_0[b]	v_e/v_0[b]	$\langle v/v_0 \rangle$[b]
Run I; 115 MeV ^{37}Cl	Pt	0.03	0.048	1.34	45.7	5.5	3.1	1.1	1.81
	W	-	0.020	1.14	54.0	8.5	3.4	1.4	2.13
Run II; 160 MeV ^{58}Ni	Pt	0.02	0.035	0.815	87.4	23.4	4.2	2.2	2.98
	W	-	0.016	0.740	97.1	27.8	4.6	2.5	3.29

a) Time taken for ion to traverse designated target layer.

b) Energies E_i (E_e) and velocities v_i/v_0 (v_e/v_0) of ions incident upon (emergent from) the Gd layer and average velocity, $\langle v/v_0 \rangle$ of ions in Gd layer; $v_0 = c/137$.

TABLE 2

TF Precession results and TF Calibration for W ions in Gd

Target Nucleus	Level	g-factor[a]	Measured Precession			
			Run I; ^{37}Cl Beam		Run II; ^{58}Ni Beam	
			$\Delta\theta$	$\Delta\theta/g$	$\Delta\theta$	$\Delta\theta/g$
^{182}W	4_1^+ [b]	0.265±0.007	32.6 ± 4.4	123 ± 17	26 ± 4	99 ± 16
^{184}W	2_1^+	0.289±0.007	32.3 ± 2.1		28.0 ± 1.9	
	4_1^+		36.1 ± 4.4		35.5 ± 4.5	
			⟨33.0 ± 1.9⟩	114 ± 7	⟨29.1 ± 1.7⟩	101 ± 6
^{186}W	2_1^+	0.312±0.011	34.7 ± 1.9		31.4 ± 1.7	
	4_1^+		38.8 ± 4.8		25.6 ± 5.3	
			⟨35.3 ± 1.8⟩	113 ± 7	⟨30.9 ± 1.6⟩	99 ± 6
				⟨114 ± 5⟩		⟨100 ± 4⟩

a) Measured g-factors from refs. [20,21,28]; see discussion in text, sect 5.1.

b) The 100 keV $2_1^+ \rightarrow 0_1^+$ transition in ^{182}W is contaminated by a transition in ^{183}W and was not included in the analysis.

TABLE 3

TF Precession Results and Measured g-factors for $^{194,196,198}Pt$

Target Nucleus	Level	Run I ^{37}Cl Beam results[a]		Run II ^{58}Ni Beam results[a]		Average g-factor[b]
		$\Delta\theta$	g	$\Delta\theta$	g	
^{194}Pt	2_1^+	35.3±1.3	0.280±0.020	35.0±1.3	0.317±0.023	0.296±0.022
^{196}Pt	2_1^+	35.2±1.5	0.279±0.021	34.6±1.5	0.314±0.024	0.294±0.023
^{198}Pt	2_1^+	36.0±3.3	0.285±0.032	33.3±3.3	0.302±0.035	0.293±0.034

a) Present measured g-factor $g = \Delta\theta/\phi$, where ϕ (Run I) = 126 ± 8 and ϕ (Run II) = 110 ± 6, see table 2 and text, sect. 5.1.

b) Weighted average value. Assigned errors are arithmetic averages of those from Runs I and II as discussed in text, sect. 5.2.

TABLE 4
Comparison of Measured Gyromagnetic Ratios in $^{194,196,198}Pt$

Isotope; Mean life[a] (ps)	$g(2_1^+)$ [b]	Method, Host (Normalization)	Reference
^{194}Pt	0.254±0.013	IPAC, Fe	Berkes et al[30]
	0.302±0.016	IPAC, Fe	Katayama et al[26]
τ=59.2±2.2	0.26 ±0.03	SF IMPAC, Fe	Kalish et al[31]
	0.294±0.021	SF IMPAC, Fe	Garber et al[32]
	0.289±0.028	SF IMPAC, Co	Garber et al[32]
	0.203±0.006	TF IMPAC, Fe (Param)[c]	Levy et al[5]
	0.280±0.020	TF IMPAC, Gd ($^{182\text{-}186}W$)	present Run I
	0.317±0.023	TF IMPAC, Gd ($^{182\text{-}186}W$)	present Run II
^{196}Pt	0.291±0.016	IPAC, Fe	Berkes et al[30]
	0.338±0.014	IPAC, Fe	Kawamura et al[33]
τ=48.3±1.4	0.28 ±0.02	SF IMPAC, Fe	Kalish et al[28]
	0.296±0.037	SF IMPAC, Fe	Garber et al[32]
	0.300±0.070	SF IMPAC, Co	Garber et al[32]
	0.311±0.028	TF IMPAC, Fe (^{194}Pt)[d]	Häusser et al[34]
	0.311±0.037	TF IMPAC, Fe (^{194}Pt)[d]	Levy et al[5]
	0.213±0.021	TF IMPAC, Fe (Param)[c]	Levy et al[5]
	0.279±0.021	TF IMPAC, Gd ($^{182\text{-}186}W$)	present Run I
	0.314±0.024	TF IMPAC, Gd ($^{182\text{-}186}W$)	present Run II
^{198}Pt	0.28 ±0.05	SF IMPAC, Fe	Kalish et al[31]
τ=33.0±1.6	0.302±0.047	TF IMPAC, Fe (^{194}Pt)[d]	Häusser et al[34]
	0.292±0.025	TF IMPAC, Fe (^{196}Pt)[d]	Stuchbery et al[17]
	0.285±0.032	TF IMPAC, Gd ($^{182\text{-}186}W$)	present Run I
	0.302±0.035	TF IMPAC, Gd ($^{182\text{-}186}W$)	present Run II

a) Mean lives from ref.[29].
b) Lifetime dependent results have been corrected for quoted mean life. Results from ref.[31] have been re-evaluated as described in sect. 5.3 of text.
c) Transient-field calibrated using the global parametrization of ref.[35].
d) Relative g-factor measurement normalized to appropriate present result.

TABLE 5

Effective boson g-factors for nuclei near A=190

Isotopes	Number of Nuclei n	g_π	g_ν	χ^2/n-2
$^{180\text{-}186}W$	4	0.81 ± 0.07	0.03 ± 0.03	0.24
$^{186\text{-}192}Os$	4	1.03 ± 0.11	-0.01 ± 0.05	1.9
^{180}W - ^{192}Os	8	0.90 ± 0.06	0.02 ± 0.02	9.7
$^{192\text{-}196}Pt$	4	0.35 ± 0.07	0.27 ± 0.03	0.60
^{180}W - ^{196}Pt	12	0.70 ± 0.15	0.11 ± 0.07	8.5
[^{176}Hf - ^{196}Pt][a]	15	0.68 ± 0.07	0.12 ± 0.03	5.0

a) From ref. [3]

Figure Captions

Fig 1. Spectrum of ^{58}Ni projectiles backscattered from the composite targe registered in the annular detector in coincidence with de-excitation γ rays during Run II. The spectral components corresponding t scattering from the Pt and W layers are labelled. This spectrur corresponds to about 75 percent of the data accumulated in Run II.

Fig. 2. Gamma-ray spectra recorded in coincidence with the Pt (upper pane and W (lower panel) regions of the backscattered particle spectrum (se fig. 1). Selected transitions are denoted by $J_i \rightarrow J_f$ and nucleus. Thes spectra represent the data recorded in the detector at +65° during Ru II.

Fig. 3. Measured (data points) and calculated (solid lines) angular correlation of de-excitation γ-rays in coincidence with backscattered beam ions fc $2_1^+ \rightarrow 0_1^+$ transitions in ^{184,186}W and ^{194,196,198}Pt during Run I (115 Me ^{37}Cl bombardment). Only the transition intensity has been adjusted t normalize the measured correlation to that calculated. For clarity presentation, the results for the various transitions have been offs from one another.

Fig. 4. As for fig. 3, but for Run II (160 MeV ^{58}Ni bombardment).

Fig. 5. Plots of $g(2_1^+)$ versus $(N_\pi - N_\nu)/N_t$ for $^{180\text{-}186}$W (top panel), $^{186\text{-}192}$O $^{192\text{-}198}$Pt and the combined data for ^{180}W to ^{198}Pt (bottom panel). Straig lines represent least-squares fits of eq. (2) to the data displayed in ea panel.

Fig. 6. Effective numbers of valence bosons N_ν^{eff} (upper panel) and N_π^{eff} (low panel) for $^{192\text{-}198}$Pt derived from the experimental $g(2_1^+)$ and $B(E2;2_1^+ \rightarrow 0_1^+)$ data as described in sect. 6 of text. Triangles represent valu derived assuming $e_\nu = 0.08$, while squares were obtained with $e_\nu = 0.1$ The solid lines indicate boson numbers obtained by "normal" counti from Z = 82 and N = 126. For neutrons, boson values counted from N 114 are also shown (dotted line). A subshell closure at N = 114 is n apparent from this analysis.

Fig. 7. Effective neutron-boson numbers and neutron-boson g-factors f $^{192\text{-}198}$Pt derived from $g(2_1^+)$ and B(E2) data as described in sect. 6 of te Values represented by triangles (squares) were obtained with $N_\pi^{eff} = 2$ (2.00) and $e_\nu = 0.08$ (0.10). In both cases $g_\pi = 0.90$ and $e_\pi = 0.22$. The so line (upper panel) indicates the number of neutron bosons counted fr N = 126. The dotted line (lower panel) shows the best-fit value of obtained for ^{180}W - ^{192}Os (see table 5).

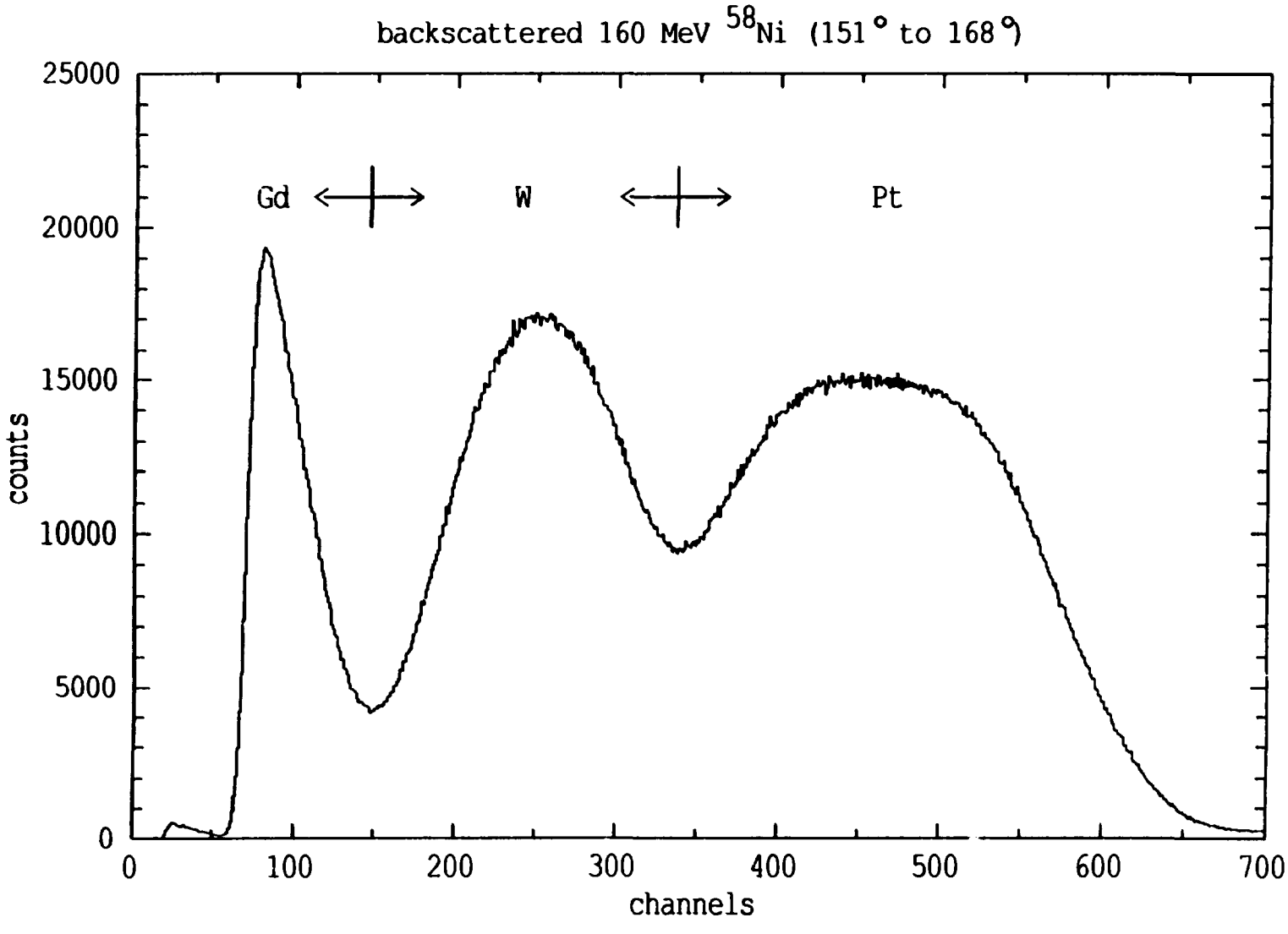
backscattered 160 MeV ^{58}Ni (151° to 168°)
Gd
W
Pt
25000
20000
15000
10000
5000
0
counts
0
100
200
300
400
500
600
700
channels

Fig. 1.

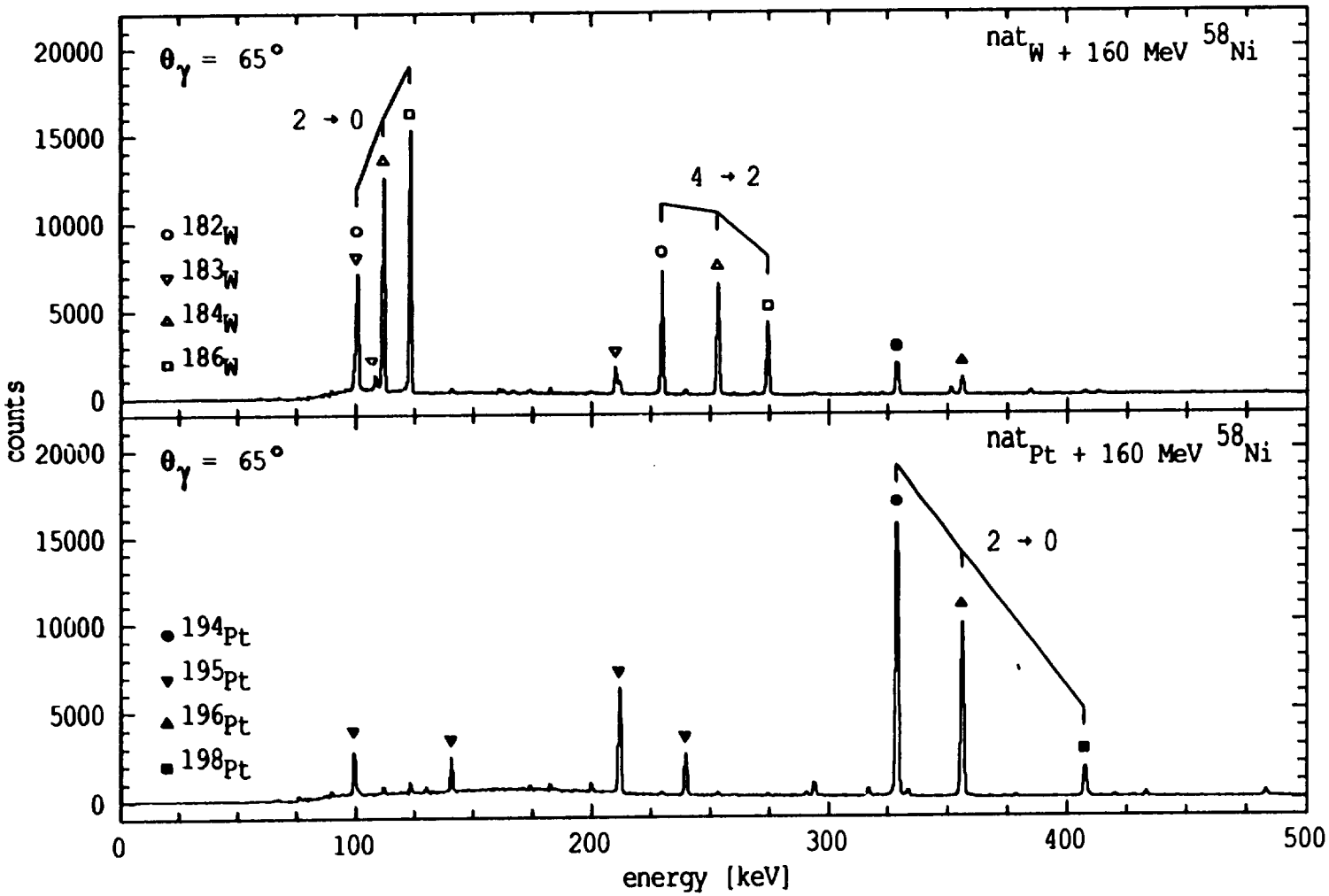
θγ = 65°
nat W + 160 MeV 58Ni
2 → 0
4 → 2
182W
183W
184W
186W
θγ = 65°
nat Pt + 160 MeV 58Ni
2 → 0
194Pt
195Pt
196Pt
198Pt
counts
energy [keV]
0
5000
10000
15000
20000
100
200
300
400
500

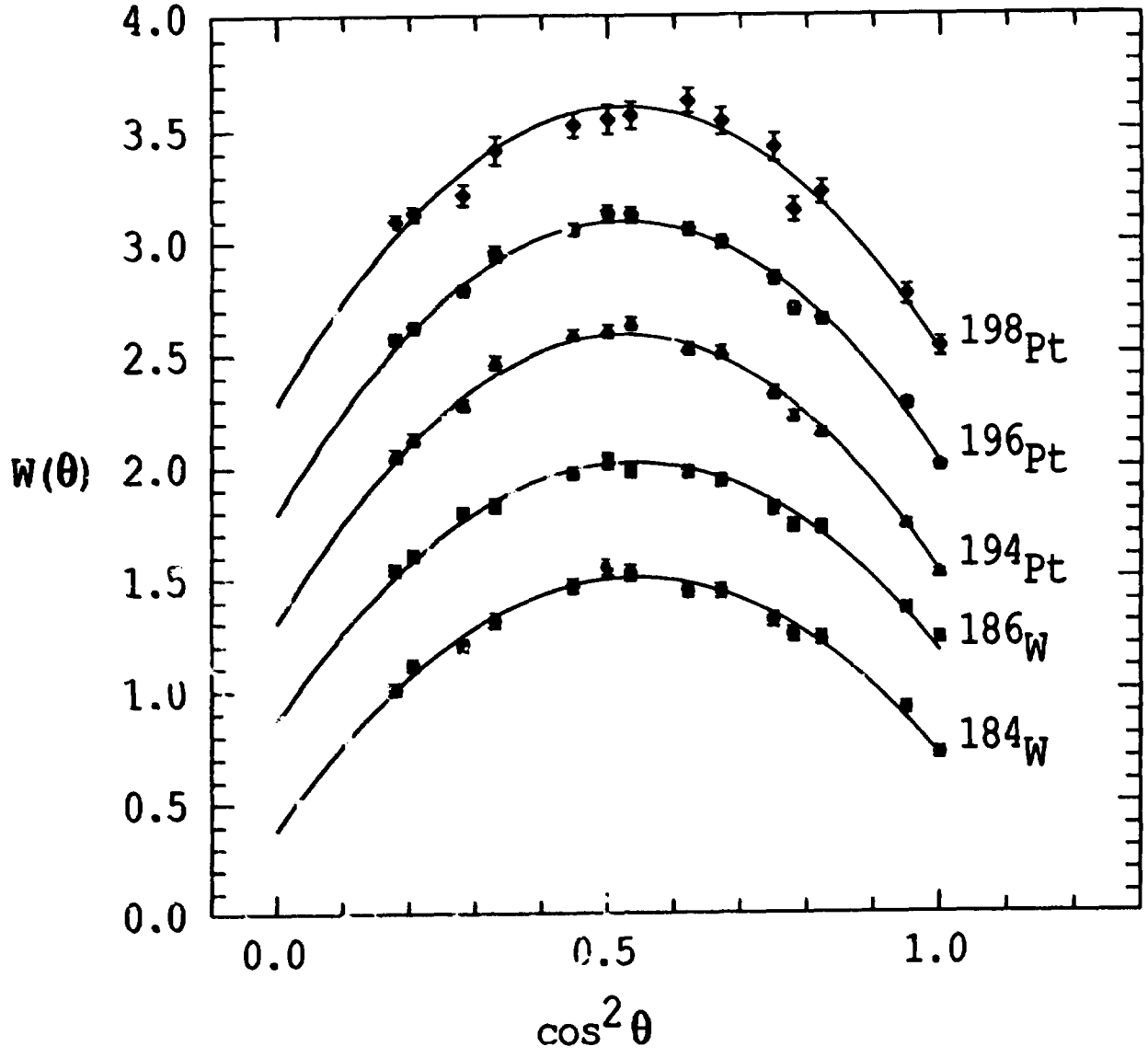
4.0
3.5
3.0
2.5
2.0
1.5
1.0
0.5
0.0
W(θ)
0.0
0.5
1.0
cos²θ
198Pt
196Pt
194Pt
186W
184W

Fig. 3

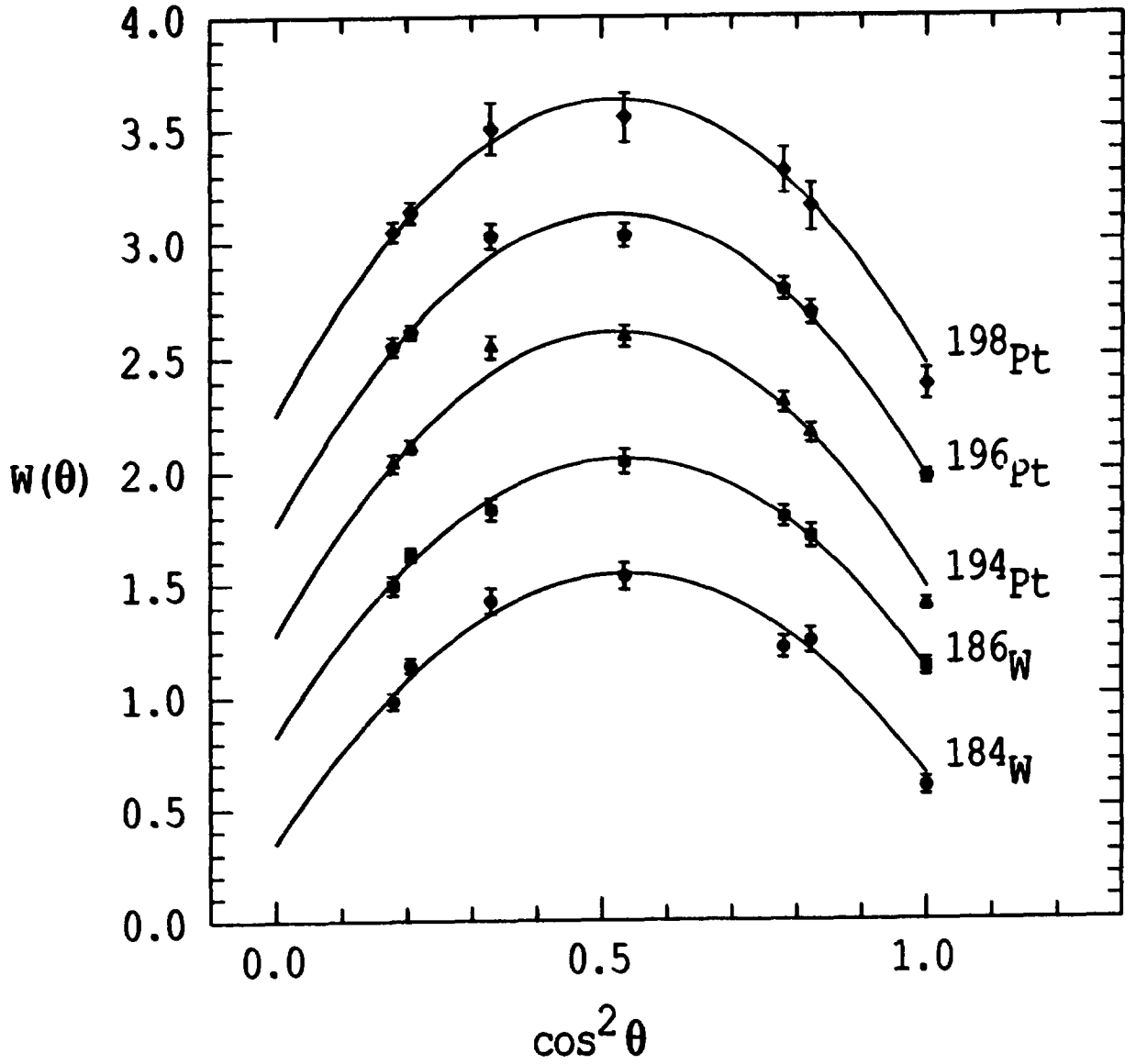
4.0
3.5
3.0
2.5
2.0
1.5
1.0
0.5
0.0
W(θ)
0.0
0.5
1.0
cos²θ
198Pt
196Pt
194Pt
186W
184W

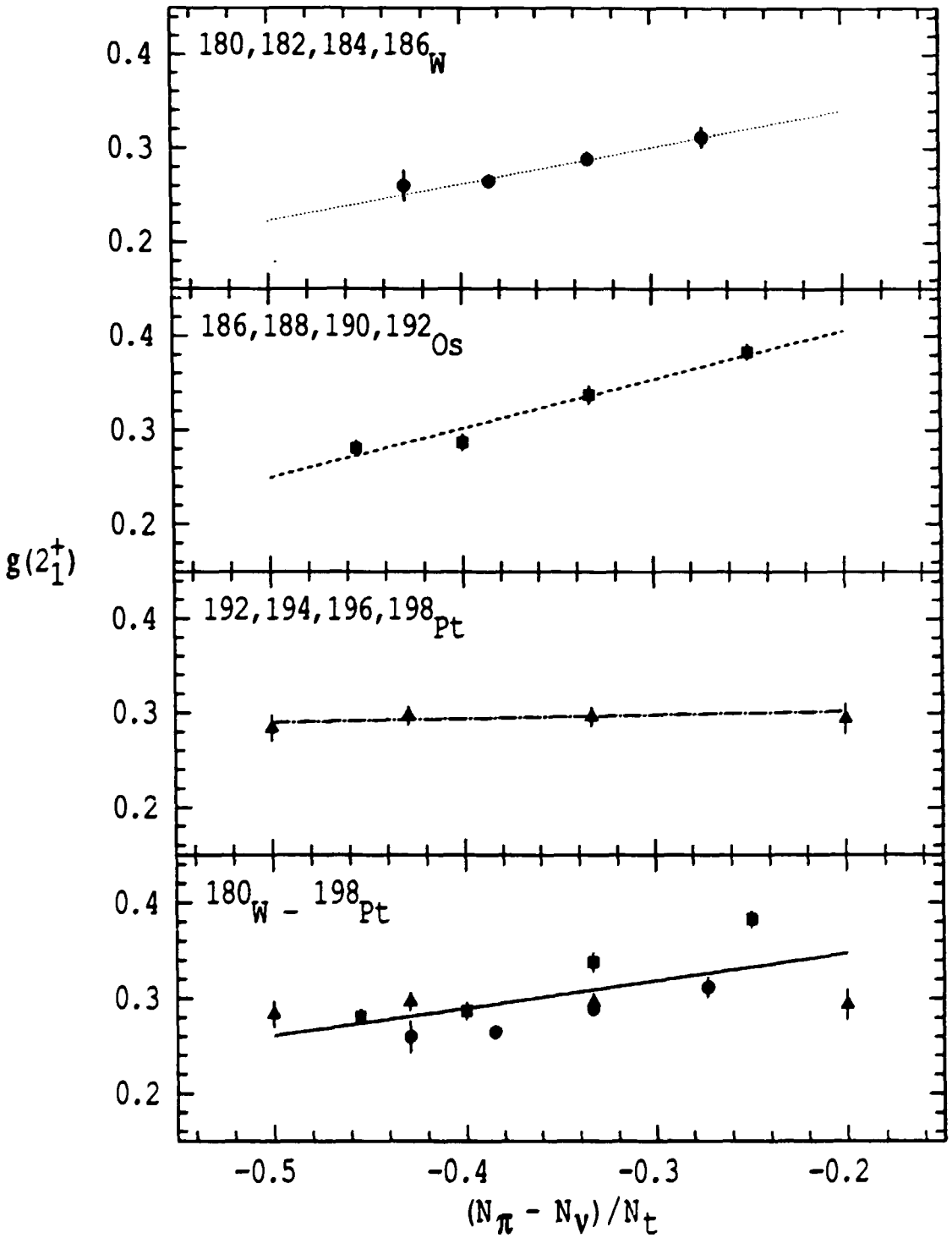
180,182,184,186W
186,188,190,192Os
192,194,196,198Pt
180W - 198Pt
g(2+1)
0.4
0.3
0.2
-0.5
-0.4
-0.3
-0.2
(Nπ - Nν)/Nt

Fig. 5

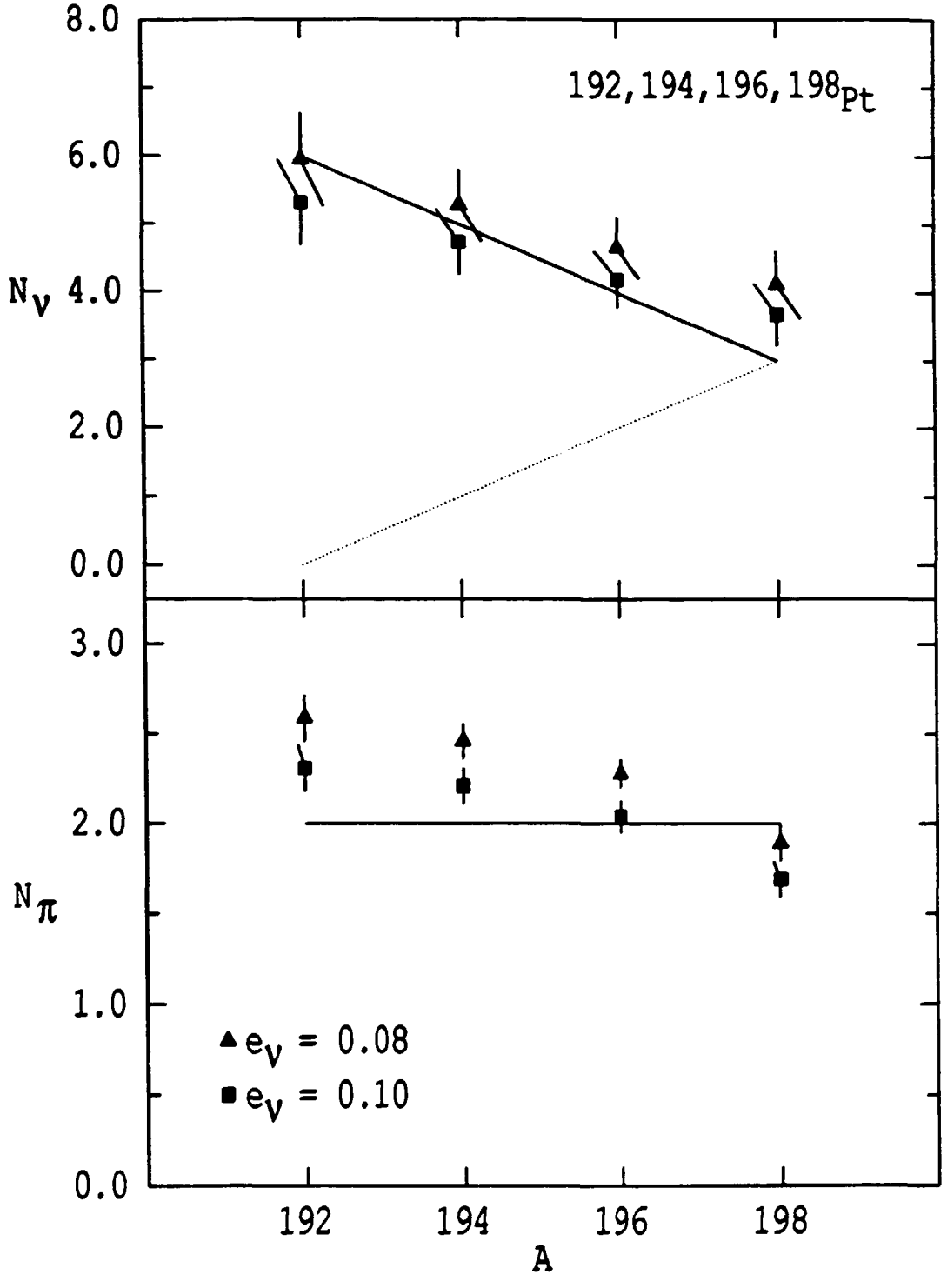
8.0
6.0
4.0
2.0
0.0
N_ν
192,194,196,198Pt
3.0
2.0
1.0
0.0
N_π
▲ e_ν = 0.08
■ e_ν = 0.10
192
194
196
198
A

Fig. 6

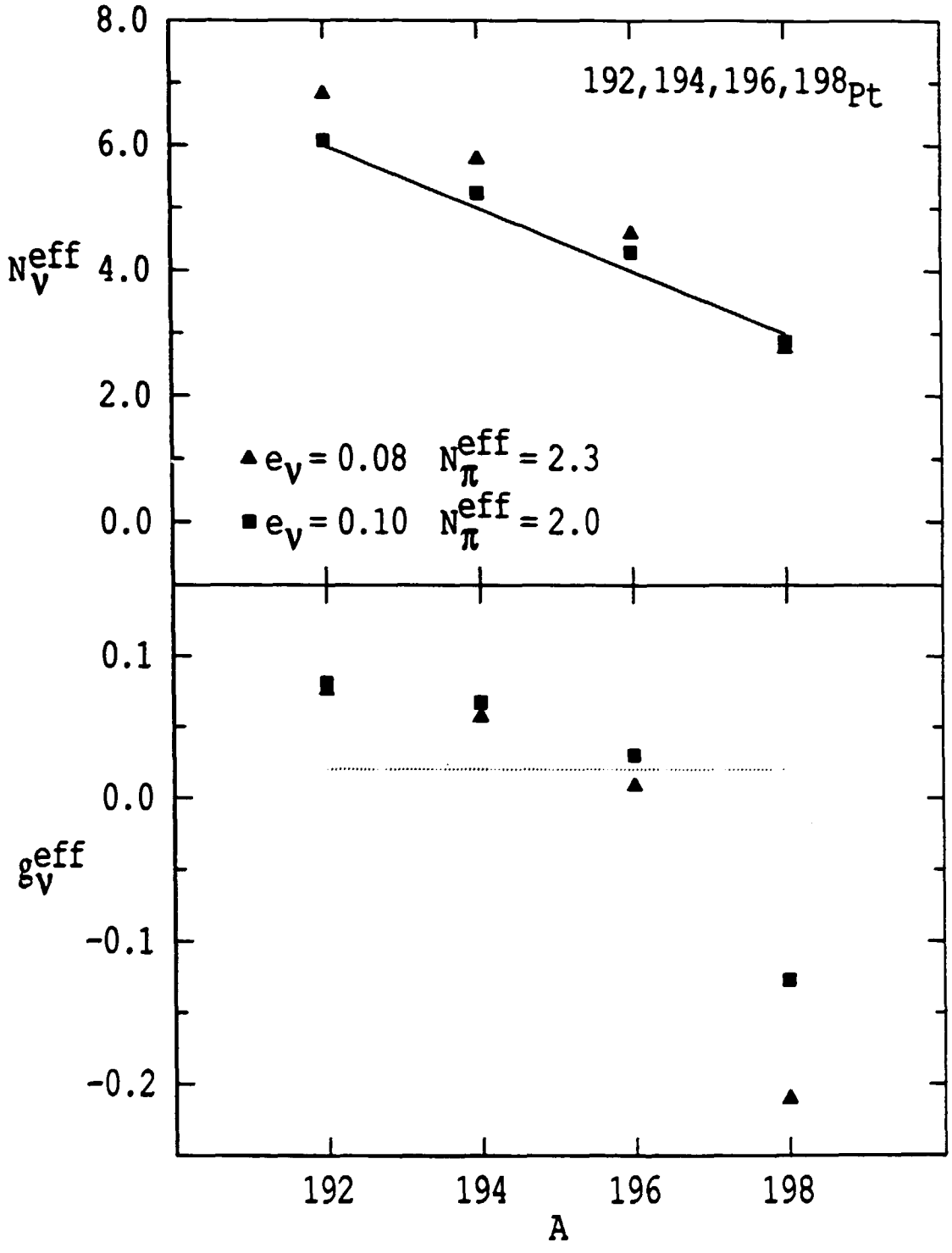
8.0
6.0
4.0
2.0
0.0
N_ν^{eff}
192,194,196,198Pt
▲ $e_\nu = 0.08$ $N_\pi^{eff} = 2.3$
■ $e_\nu = 0.10$ $N_\pi^{eff} = 2.0$
0.1
0.0
-0.1
-0.2
g_ν^{eff}
192
194
196
198
A

Fig. 7.